1604 *KSME International Journal, Vol. 16 No. 12, pp. 1604~1612, 2002*

A Study on the Fault Diagnosis of Roller-Shape Using Frequency Analysis of Tension Signals and Artificial Neural Networks Based Approach in a Web Transport System

Kyung-Mo Tahk*
Satellite Technology Research Center, KAIST, Daejeon 305-701, Korea
Kee-Hyun Shin
School of Mechanical and Aerospace Engineering, Konkuk University, Seoul 143-701, Korea

Rollers in the continuous process systems are ones of key components that determine the quality of web products. The condition of rollers (e.g. eccentricity, runout) should be consistently monitored in order to maintain the process conditions (e.g. tension, edge position) within a required specification. In this paper, a new diagnosis algorithm is suggested to detect the defective rollers based on the frequency analysis of web tension signals. The kernel of this technique is to use the characteristic features (RMS, Peak value, Power spectral density) of tension signals which allow the identification of the faulty rollers and the diagnosis of the degree of fault in the rollers. The characteristic features could be used to train an artificial neural network which could classify roller conditions into three groups (normal, warning, and faulty conditions). The simulation and experimental results showed that the suggested diagnosis algorithm can be successfully used to identify the defective rollers as well as to diagnose the degree of the defect of those rollers.

Key Words : Web, Web Transport System, Web Tension, Roller/Roll, Fault Diagnosis, Artificial Neural Network

Nomenclature

T : Change in the web tension from a steady-state operating value
V : Change in the web velocity from a steady-state operating value
v : Steady-state operating value of web velocity
E : Young's modulus
A : Cross-sectional area of web
L : Length of web
J : Polar moment of inertia of roller
R : Radius of roller
b : Rotary friction constant of bearing
τ : Change in driving torque of motor
e : Eccentricity of roller
f : Frequency, Non-linear activation function
f_n : Dither frequency due to the eccentric roller
ω : Angular velocity of roller
h : Web thickness
P : Rotating period of roller, Period of tension signal
N : Number of time domain samples
n : Time domain sample index
k : Frequency domain index
W : Weighting factor
G : Balance quality grade
v_{n_ref} : Operating velocity
ΔV : Magnitude of velocity variation caused by roller eccentricity

* Corresponding Author,
E-mail : tgm@satrec.kaist.ac.kr
TEL : +82-42-869-8622; **FAX** : +82-42-861-0064
Satellite Technology Research Center, KAIST, Daejeon, 305-701, Korea. (Manuscript **Received** January 9, 2002; **Revised** September 26, 2002)

1. Introduction

The web is a flat and flexible material such as

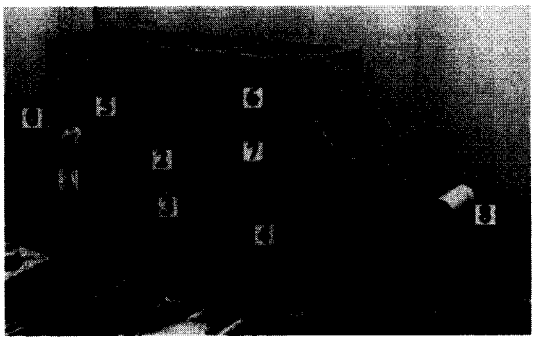

(0 : Unwinding roll, 1~4 : Idle roller, 5 : Load cell, 6 : Driven roller, 7 : Load cell, 8 : Winding roll)

Fig. 1 A typical web transport system

paper, steel plate, plastic film, etc. It is usually transported by many driven and idle rollers and is under the tension as it is manufactured or processed in several consecutive processing sections. Figure 1 shows a typical web transport system, which uses a polypropylene film of 14 μm thickness.

In many web processes, there are so many kinds of tension disturbance sources such as the contact of a nip roller on a moving web. One of significant disturbance sources during the processing of a web includes such as roller defects. The periodic disturbances due to the eccentric roller can create significant tension variations in the web span in multi-span web transport systems (Tahk and Shin, 1999 ; Shin, 2000 ; Roisum, 1996). Thus, it is important to monitor and diagnose the defects of rollers such as excessive eccentricity and runout in order to minimize the degradation of product quality and economic loss.

In this paper, a new diagnosis algorithm is suggested to detect the defective rollers based on the frequency analysis of web tension signals and artificial neural networks technology. The proposed diagnosis algorithm will be validated experimentally by using the prototype web transport system shown in Fig. 1.

2. Theoretical Background

A mathematical model for the multi-span web transport system in Fig. 2 can be obtained by combining the model for each primitive element

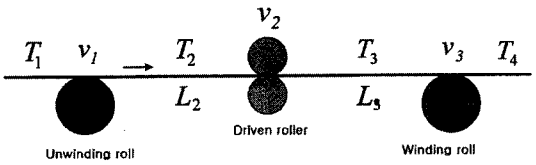

Fig. 2 A two-span web transport system

(Shin, 1991). The mathematical tension model can be written as follows.

2.1 Tension-web velocity relationship

Equations (1) and (2) represent a linearized dynamic tension model for the web transport system when there is no slippage between the web material and the rollers/rolls.

$$\frac{dT_2}{dt}=-\frac{\nu_2}{L_2}T_2+\frac{\nu_1}{L_2}T_1+\frac{A_2E_2}{L_2}[V_2-V_1] \quad (1)$$

$$\frac{dT_3}{dt}=-\frac{\nu_3}{L_3}T_2+\frac{\nu_2}{L_3}T_2+\frac{A_3E_3}{L_3}[V_3-V_2] \quad (2)$$

2.2 Tension-tangential velocity of roller relationship

A relationship between the tension and the tangential velocity of the roller can be obtained from the torque balance on the roller as follows :

$$\frac{d}{dt}[V_2(t)] =-\frac{bV_2(t)}{J_2}+\frac{R_2^2}{J_2}[T_3(t)-T_2(t)]+\frac{R_2}{J_2}\tau_2 \quad (3)$$

2.3 Tension-roller velocity relationship

In order to determine the influence of the roller shape on the web tension due to the variation of roll radius, it needs to know the correlation between the roller surface velocity and the web velocity. The following description with Eqs. (1), (2) and (3) provides the relationship between tension variation and diameter variation of roller.

$$V_{roller}=R\frac{2\pi}{P} \quad (4)$$

$$V_{web}=\left(R+\frac{h}{2}\right)\frac{2\pi}{P} \quad (5)$$

From Eqs. (1) ~ (5), it is clear that the variance of roller radius causes tension variation. Based on the facts described above, the roller defects can be detected by the analysis of web

tension signals in the frequency domain.

2.4 Frequency analysis

In this paper, the fast Fourier transform of the sampled web tension signals is used to analyze frequency characteristics of web tension signals. The fast Fourier transform (Irvine, 1998) $F(k)$ for a discrete-time web tension $T(n)$ can be written as:

$$F(k)=\frac{1}{N}\left[\sum_{n=0}^{\frac{N}{2}-1}\{T(2n)W^{2nk}\}+W^{k}\sum_{n=0}^{\frac{N}{2}-1}\{T(2n+1)W^{2nk}\}\right] \quad (6)$$

where

$$k=0,\ 1,\ \cdots,\ N-1,\ W^{m}=\exp(-j2\pi\ \mathrm{m/N})$$

2.5 Artificial neural network

An artificial neural network (ANN) consists of a number of richly interconnected artificial processing neurons called nodes, collected together in layers forming a network. A typical ANN is schematically illustrated in Fig. 3. The number of nodes within the input and output layers are dictated by the nature of the problem to be solved and the number of input and output variables needed to define the problem. The number of hidden layer and nodes within each hidden layer is usually a trial and error process. Each node in a layer provides the threshold of a single value by summing up their input value (X_i) with the corresponding weight value (W_i). Then the NET value is formed by adding up this single value, with the bias term (θ_i). The NET is then further processed by the non-linear activation function (f), providing an output value (OUT) (Paya, 1997) which is defined as

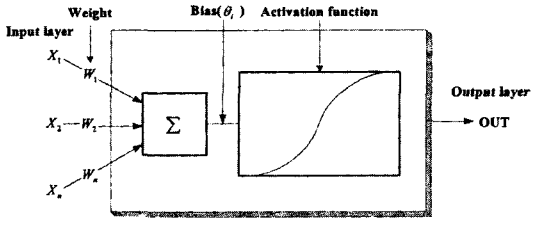

Fig. 3 Operation of artificial neuron in a layer

$$OUT=F(NET)=f\left(\sum_{i=1}^{n}W_iX_i+\theta_i\right) \quad (7)$$

The training of ANN is carried out by utilizing the most commonly used algorithm known as back-propagation networks (BPN) (Paya, 1997). The BPN uses the normalized sum square error to adjust the value of the weights on the neural connection in the multiple layer. In this paper, the input characteristic features of tension signal were normalized by using the maximum among the features and used for input variables of ANN. The output decisions of ANN are used to classify the roller conditions such as normal, warning and faulty conditions.

2.6 Feature extraction for fault diagnosis

It is not suitable for direct classification of roller condition by using the time series tension signals. Therefore, it is necessary to extract time invariant features from the time and frequency domain for input to the classifier (BPN). To fulfill the work of diagnosis using output decision of the BPN, some characteristic features of sampled tension signals are used.

There are several ways to represent about the maximum variation of the tension signals. In this paper, the peak value and mean square value of tension signals in time domain are used for the input features of the artificial neural network. The mean square value $\overline{T^2}$ of tension signals is approximated by time average, if it is assumed that the tension signal $T(t)$ is stationary (Harris, 1995):

$$\overline{T^2}=\frac{1}{P}\int_0^P T^2(t)\,dt \quad (8)$$

In addition, the power spectral density $W(f)$ of tension signals in frequency domain is also used for the input features of the artificial neural network. The power spectral density is defined as the mean square response of an ideal narrow-band filter to tension signal $T(t)$, divided by the frequency bandwidth Δf of the filter in the limit as $\Delta f \to 0$ at frequency(Hz) (Harris, 1995):

$$W(f)=\lim_{\Delta f\to 0}\frac{\overline{T_{\Delta f}^2}}{\Delta f} \quad (9)$$

Table 1 Balance quality grades (from ISO 1940)

Quality grade (G)	Applications
1.0	High speed precision hard nips
2.5	>2000 MPM transport system >1000 MPM nipped process rollers
6.3	Most web machine rollers
16	Low speed (<30 MPM) web roller

Table 2 Thresholds for fault diagnosis of roller-shape

Roller condition	Quality grade (G)
Normal	$G \leq 4.0$
Warning	$4.0 < G \leq 6.0$
Fault	$G > 6.5$

2.7 Determination of thresholds

The eccentric roller would cause severe vibration when driven against a tremendous web flutter and tension surges. Thus, most rollers which operate more than 30 MPM should be dynamically balanced to a specific criteria. One common standard is ISO 1940. In this paper, the balance quality grades (Roisum, 1996) (from ISO 1940) are used for thresholds which classify the roller conditions such as normal, warning, and faulty condition. The grade of balance quality is termed G where

$$G = e \cdot \omega \tag{10}$$

These balance quality grades are listed on charts as shown in Table 1. In this section, the three thresholds to be applied to fault diagnosis of roller-shape are determined by the authors of this paper using quality grade and are as Table 2.

3. The Proposed Diagnosis Algorithm for a Roller-Shape Fault

A new diagnosis algorithm to detect the roller shape fault without any additional diagnosis instruments is proposed. It is assumed that the web tension is controlled within the desired limit value and there are no faults in the tension measurement instruments (e.g. load cells, I/O board, etc.). The diagnosis algorithm can be outlined as follows and the flowchart of that is shown in Fig. 4.

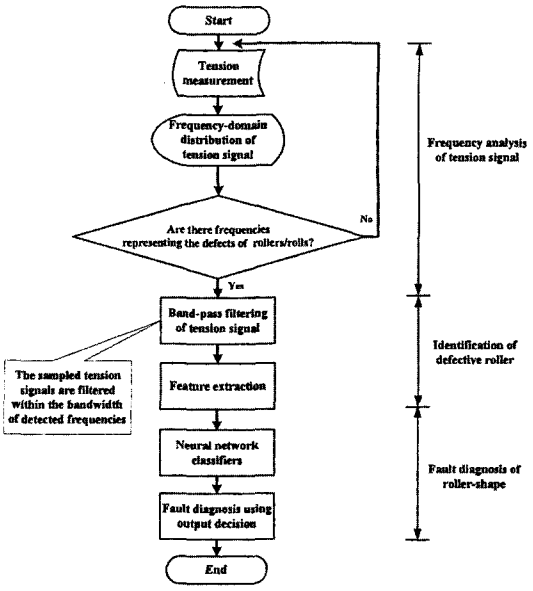

Fig. 4 The flowchart of roller-shape fault diagnosis

Diagnosis algorithm

Step 0 (Tension measurement) : The web tension $T(t)$ is measured from load cell in each span.

Step 1 (Fast Fourier transform) : The sampled tension signals are transformed into the frequency domain by using FFT.

Step 2 (Identification of frequencies representing the defects of rollers) : The frequency components of tension signal corresponding to the defective rollers are identified by using the result of step 1.

Step 3 (Band-pass filtering) : For the purpose of estimating the effect of faulty roller on the tension variation, the sampled tension signals are filtered within the bandwidth of detected frequencies in step 2.

Step 4 (Calculation of characteristic features) : The characteristic features of filtered tension signals for the diagnosis of roller faults are obtained from the features of tension signals (refer to the section 2.6).

Step 5 (Detection of the faulty roller) : By comparing the magnitude of the features of

the tension signals, the defective rollers are identified in a case of the rollers have the same radius. The very upstream roller of the span whose tension has biggest features is defective.

Step 6 (Classification of roller condition) : The characteristic features obtained from step 4 are used to classify the following three different roller conditions by using ANN.
- Normal condition
- Warning condition
- Faulty condition

Step 7 (Fault diagnosis) : Fault diagnosis is carried out using the output decision of ANN.

4. Simulations for the Algorithm Verification

In order to examine the performance of proposed diagnosis algorithm, a simulation study for a typical web transport system (Fig. 5) has been carried out. This system includes eccentric rollers (1^{st}, 3^{rd} roller) for the test. The simulations were performed with following scheme. Simulation parameters are shown in Table 3.

Table 3 Simulation Parameters

Simulation Parameters	Values
Dither frequency (f_1, f_3)	4 Hz
Eccentricity (e_1) of the 1^{st} roller	0.00012 m
Eccentricity (e_3) of the 3^{rd} roller	0.00026 m
Operating velocity	1 m/s
Velocity variation (V_1)	$1+0.003\sin(2\pi f_1 t)$ m/s
Velocity variation (V_3)	$1+0.0065\sin(2\pi f_3 t)$ m/s

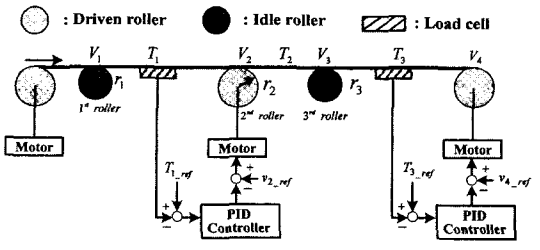

Fig. 5 A simplified web transport system

- It is assumed that there is no slippage between rollers and web materials.
- The basic mathematical models for simulation are Eqs. (1)~(5).
- To generate the effect of roller eccentricity, the dither signal is inserted into the models for the 1^{st} and 3^{rd} idle roller. And dither signal has the form,

$$V_n = v_{n\_ref} + \Delta V_n \sin(2\pi f_n t) \qquad (11)$$

- The tension and speed of the web material are controlled within the desired limit value.
- The tension signals T_1 and T_3 are calculated by using Eqs. (1)~(5) and (11).

4.1 Simulation results

Figure 6 shows that the suggested algorithm identifies the eccentric rollers (1^{st}, 3^{rd} roller) in the web transport system. Figure 7 shows the effect of eccentric rollers on tension variation in the time domain. Table 4 shows the characteristic features calculated in step 4. In Table 4, the characteristic features of T_3 are larger than those of T_1. It means that the 3^{rd} roller has larger eccentricity than that of the 1^{st} roller. From Table 4, it may be concluded that the faulty roller (3^{rd} roller) is detected by comparing the magnitude of characteristic features of T_1 with those of T_3.

Table 5 shows a recognition success rate for three conditions of step 5 in the algorithm. In this

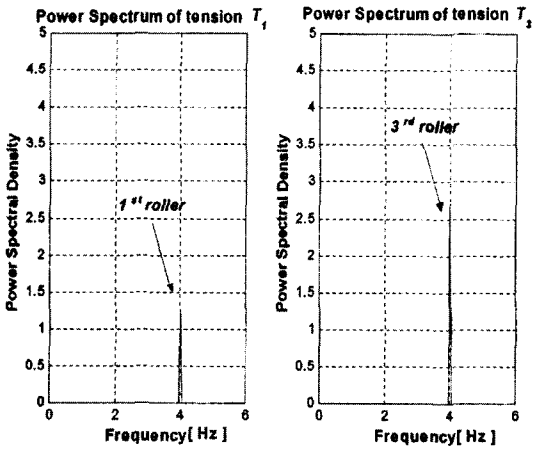

Fig. 6 Frequencies of tension signal due to the defective rollers/rolls

step, ninety sets of the characteristic features were used to test the classification performance of the back-propagation neural networks. The thresholds of each condition are based on the roller balance quality grade. According to the diagnosis results of the 1st and 3rd rollers based on the characteristic features calculated in step 4, the conditions of the 1st and 3rd roller were classified respectively into the normal condition and fault condition. The back-propagation neural networks were found to have recognition success of 96.66% in average. All the neural networks have three-input and three-output neurons.

Table 4 Characteristic features calculated in step 4

Characteristic features	T_1	T_3
Mean square value	0.0263	0.0752
Peak value	0.0686	0.3243
Power spectral density	1.23	2.73

Table 5 Classification results based on the input characteristic features at the same condition

Roller condition	Correctly classified
Normal	100%
Warning	95%
Fault	95%
All	96.66%

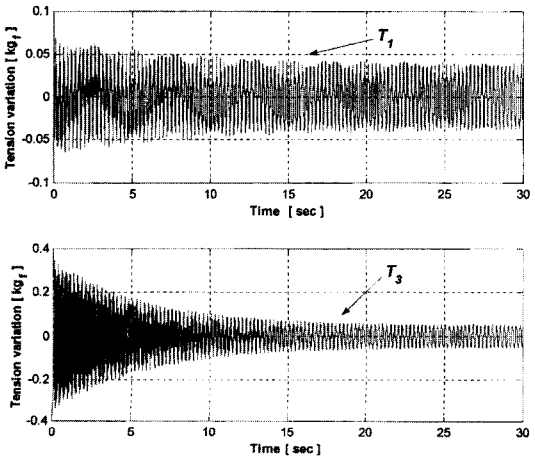

Fig. 7 Tension variations due to the eccentric rollers

5. Experimental Evaluation

5.1 Experimental setup

Figure 8 shows the experimental system configuration. It consists of an unwinding roll, the driven/non-driven rollers and a winding roll. In this system, four load cells are mounted to measure the tension T_1 and T_3. Three AC motors are used to drive the driven rollers/rolls. The motors are controlled in real-time by using the Vxworks® real-time system and force targ et boards. The tension signals were sampled at 200 Hz using A/D converter fitted to a SUN SPARC STATION and the tension signals taken by the load cells were then digitally filtered by a low-pass filter.

The sampled tension signals in each span are transformed from the time domain to the frequency domain and used to detect the defective rollers and to estimate the degree of defects by the algorithm proposed. The MATLAB 5.1 was used for this analysis. The experiment was conducted with the experimental parameters shown in Table 6.

Table 6 Experimental parameters

Experiment Parameters	Values
Dither frequencies of two rollers	4 Hz
Eccentricity of No. 1 roller	0.00012 m
Eccentricity of No. 3 roller	0.00020 m
Operating velocity	1 m/s

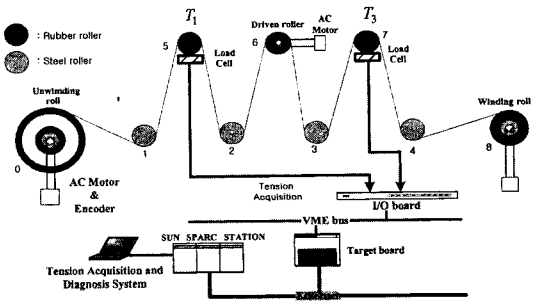

Fig. 8 Schematic diagram of fault diagnosis system

5.2 Experimental results and discussions

5.2.1 Frequency analysis of tension signals

Table 7 contains the radius of rollers and rolls as well as the frequency characteristics of tension signals that are induced by faulty rollers/rolls in the case of ν=0.5, 1 m/s in this experiment.

As shown in Table 7, the tension signal that has the specific frequencies representing the defects of the rotating rollers is shown to be generated by roll/roller faults. The power spectrum of the measured tension due to the fault of rollers/rolls are shown in Figs. 9 and 10.

Figure 9 shows the frequencies of tension signals T_1 and T_3 against the power spectral density in the case of ν=0.5 m/s and $t_1=t_3$=4 kgf (operating tension). In this case, the tension T_1 is measured from the load cell installed with No. 5 rubber roller (see Fig. 8). Therefore, considering the correlation between the transporting direction of web, the position in which the load cell is placed and the rotating frequencies of several rolls and rollers, the frequency component in range of 1.4 Hz is likely to occur by the eccentricity of No. 0 unwinding roll. On the other hand, tension T_3 is measured in the load cell which equipped with No. 7 rubber roller.

In particular, as shown in Figs. 9 and 10, the tension frequencies of steel and rubber roller (see the case of No. 3 and No. 6 roller) which is not changed during winding process became doubled, if the operating velocity of web became twice as fast as ν=0.5 m/s. From these facts described above, it is seen that the results of frequency analysis of tension signals allow us to identify the defective rolls/rollers during winding process.

Table 7 Frequencies of tension variation according to operating velocity and roller radius

Operating conditions / Rollers	Operating Velocity (m/s)			
	0.5		1.0	
	R(m)	f(Hz)	R(m)	f(Hz)
No. 8	0.094	0.8	0.055	2.9
No. 0	0.056	1.4	0.094	1.7
No. 1, 2, 3, 4	0.040	2.0	0.040	4.0
No. 5, 6, 7	0.050	1.6	0.050	3.2

5.2.2 Tension variation due to the eccentric roller

From the experimental results in section 5.2.1, it is noted that the eccentric roller could be identified by the frequency analysis of sampled tension signals. However, the key factors for the fault diagnosis of roller-shape such as the eccentricity of roller and effect of eccentric roller on the tension variation could not be extracted from the above results. Then, it is necessary to

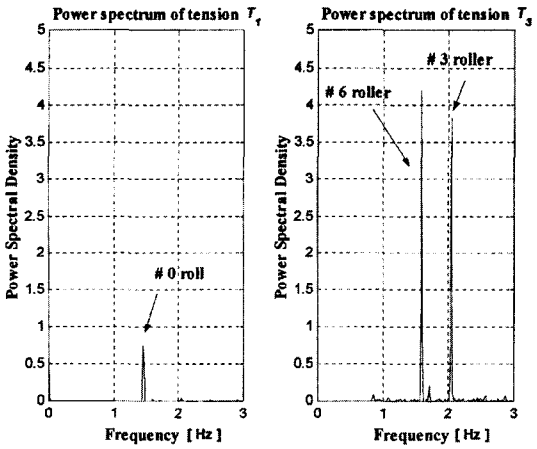

Fig. 9 Frequencies of tension signal due to the defective rollers/rolls (ν=0.5 m/s, $t_1=t_3$=4 kgf)

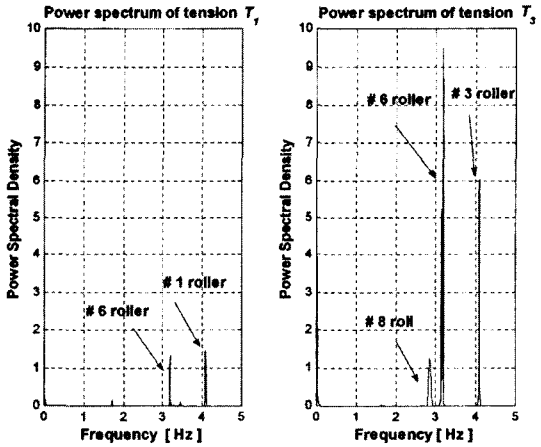

Fig. 10 Frequencies of tension signal due to the defective rollers/rolls (ν=1 m/s, $t_1=t_3$=4 kgf)

know the relationship between the eccentricity of roller and tension variation induced by the eccentric roller. This relationship can be obtained by analyzing the filtered tension signals within the bandwidth of the identified frequencies.

Figures 11 and 12 show the tension variation in the case of $\nu=1$ m/s and $t_1=t_3=4$ kgf. Figures 13 and 14 depict respectively the filtered tension of T_1 and T_3 in the range of $f=4$ Hz. Table 8 shows the relationship between eccentric quantities of rollers and maximum tension variation ($T_{v/max}$) obtained by experimental results, where the $T_{v/max}$ is a maximum tension variation in the range of 10 sec to 70 sec and the e_c is the mean value of the eccentricity measured on the four points of each roller.

As shown in Table 8, one should note that the more eccentricity of roller is raised, the more tension variation is generated by the eccentric roller.

Table 8 Relationships between eccentric quantities of rollers and maximum tension variation

# of roller / Eccentric quantities	No. 1 roller	No. 3 roller
f(Hz)	4	4
e_c(mm)	0.12	0.20
$T_{v/max}$(kgf)	0.11	0.23

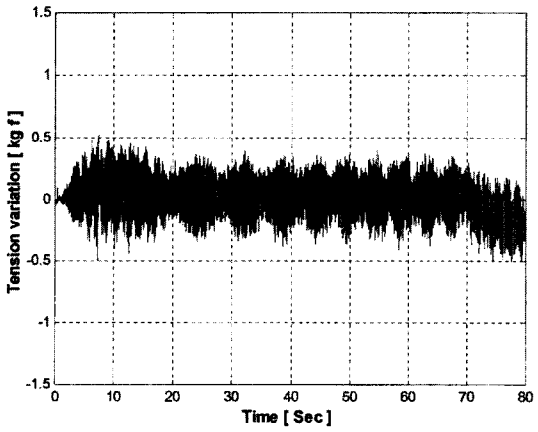

Fig. 11 Tension variation T_1 in the case of $\nu=1$ m/s, $t_1=t_4=4$ kgf

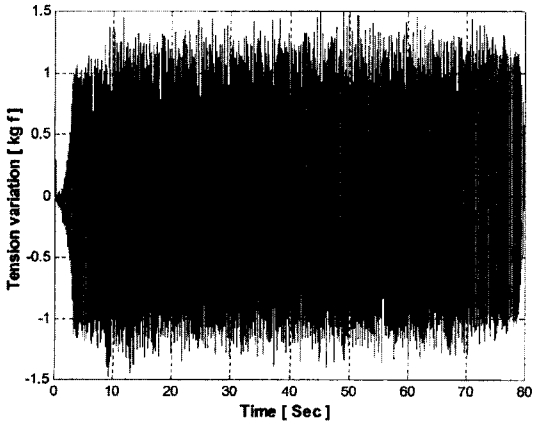

Fig. 12 Tension variation T_3 in the case of $\nu=1$ m/s, $t_1=t_3=4$ kgf

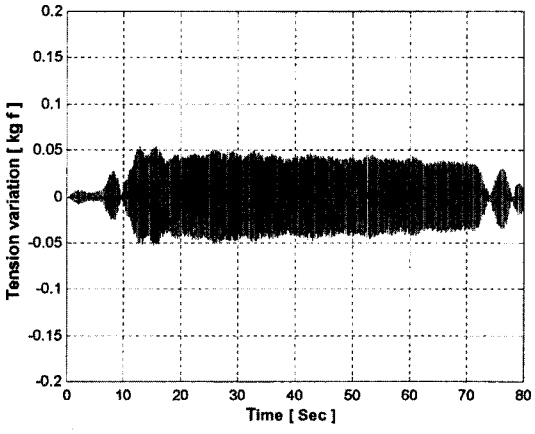

Fig. 13 Tension variation T_1 due to the eccentric No. 1 roller ($f=4$ Hz, $\nu=1$ m/s)

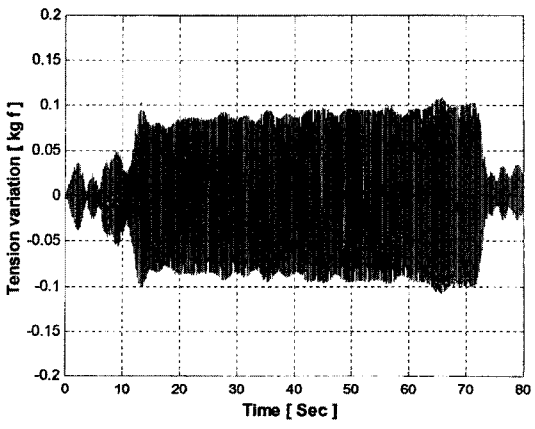

Fig. 14 Tension variation T_3 due to the eccentric No. 3 roller ($f=4$ Hz, $\nu=1$ m/s)

Table 9 Results of features extracted

Characteristic features	T_1	T_3
Mean square value	0.0306	0.0622
Peak value	0.0540	0.0995
Power spectral density	1.4658	5.9417

Table 10 Classification results based upon input features at the same condition

Roller condition	Correctly classified
Normal condition	100%
Warning condition	100%
Faulty condition	95%
All	98.33%

5.2.3 Fault diagnosis of roller shape

In order to detect roller faults, the feature extraction was carried out using the characteristic features of tension signals. By comparing the results of features extracted, the eccentric roller was detected even in the case of two rollers (No. 1, No. 3 rollers) with the same radius in the web transport system.

The results of feature extraction are shown in Table 9. The artificial neural network was trained using a variety of architectures. All the networks have three-input and three-output neurons. Networks with one hidden layer were trained for up to 20 hidden neurons and a variety of two hidden layer networks were also trained. The classification of roller condition based on the characteristic features was carried out using experimental data. The recognition success rate is shown in Table 10.

6. Conclusions

This paper proposes a new diagnosis algorithm of roller shape faults. The frequency domain analysis of web tension signals has been used to detect faulty rollers. The characteristic features of sampled tension signals have been applied to artificial neural network in order to classify the condition of rollers. Simulations and experiments were conducted in several conditions of the web transport system to examine the performance of the proposed diagnosis algorithm. The advantages of the suggested algorithm are as follows:

(1) The faulty rollers are detected in the multi-span web transport system that included rollers having even the same radius without any additional diagnosis instruments.

(2) The conditions of rollers are classified into three conditions. The classification success rate was very high : 98.33%.

Thus, a large-scale web transport system which might have rollers with same radius seems to be effectively monitored and diagnosed by using the suggested algorithm.

Acknowledgment

This research has been partially supported by Konkuk university in 1999.

References

Harris Cyril M., 1995, "Shock and Vibration Handbook-Fourth Edition," McGRAW-HILL, pp. 11.5~11.8.

Tom Irvine, 1998, "The Fast Fourier Transform," Vibrationdata Company Technical paper.

Paya B. A., 1997, "Artificial Neural Network Based Fault Diagnosis of Rotating Machinery Using Wavelet Transforms as a Preprocessor," *Mechanical Systems and Signal Processing*, Vol. 11, No. 5, pp. 751~765.

Roisum David R., 1996, "The Mechanics of Rollers," TAPPI PRESS, pp. 11~20.

Shin Kee-hyun, 2000, "Tension Control," TAPPI PRESS, pp. 20~24.

Tahk Kyung-mo and Shin Kee-hyun, 1999, "A Study on the Fault Diagnosis of Roller-Shape using Frequency Domain Analysis of Web Tension Signals," *Proc. of Manufacturing & Design Conference of the KSME*, pp. 338~343.